Journal of Advanced Marine Engineering and Technology, Vol. 49, No. 6, pp. 457~462, 2025
J. Advanced Marine Engineering and Technology (JAMET)
https://doi.org/10.5916/jamet.2025.49.6.457

ISSN 2234-7925 (Print)
ISSN 2765-4796 (Online)
Original Paper

Analyzing cut-edge corrosion in hot dip galvanized and Zn-Al-Mg alloy using image processing

Yeonwon Kim[1] · Sang-Du Yun[2] · Inyoung Park[3] · Beomsoo Kim[4] · Jeonghyeon Yang[†]

(Received October 10, 2025 ; Revised November 5, 2025 ; Accepted December 30, 2025)

Abstract: Currently, hot-dip galvanized steel is widely used because of its ability to provide effective corrosion resistance at a relatively low cost. However, there is a growing demand for materials that can enhance the corrosion resistance while maintaining the coating thickness, particularly in harsh environments. The development of Zn-Al-Mg alloys aims to address this need by improving the corrosion resistance of Zn coatings. The Zn-Al-Mg alloy is designed to offer enhanced protection against corrosion, even in vulnerable areas, such as the cut-edge region, where traditional zinc coatings may be weaker. To precisely assess the protective capability, the specimens were subjected to cyclic corrosion tests. The cut-edge area was meticulously observed using scanning electron microscopy and energy-dispersive X-ray spectroscopy. Additionally, advanced image processing techniques were employed to determine the detectability and extent of corrosion in the cut-edge area. This comprehensive evaluation aims to provide valuable insights into the effectiveness of Zn-Al-Mg alloy coatings in enhancing corrosion resistance and to inform better material selection for applications in harsh environments.

Keywords: Corrosion resistance, Zn-Al-Mg alloy, Cut-edge, Image processing technique

1. Introduction

Galvanization is widely recognized as one of the most practical and effective technologies for protecting steel from corrosion and is extensively used in various industrial fields, including the construction, automotive, and marine industries **[1]**. Galvanization involves the application of a zinc coating to steel, which forms a zinc-based corrosion-product layer on the steel surface. This layer acts as a physical barrier against environmental elements and functions as a sacrificial anode. The sacrificial anode effect indicates that the Zn layer will corrode preferentially over the underlying steel, thereby forming a passive layer that effectively protects the steel from corrosion **[2]**.

Zn-Al-Mg (ZAM) alloy coatings have been developed to further enhance the corrosion protection provided by conventional galvanization. The addition of Al and Mg promotes the formation of stable corrosion products and improves the barrier protection, particularly at the cut edges. Consequently, ZAM-coated steels are widely used in construction, automotive, marine, and infrastructure applications where long-term durability is required, offering superior cut-edge corrosion resistance compared with conventional zinc coatings.

A common issue with galvanized steel is cut-edge corrosion during use **[3]**. Cut-edge corrosion typically occurs when steel, which is produced and transported in sheet form, is cut to the required size for various applications. This cutting process exposes the untreated cut edges that are not covered by a protective zinc coating. These exposed edges are resistant to corrosion, often at a faster rate than the coated areas **[4]**. This phenomenon affects not only galvanized steel but also other steel and alloy sheet materials and is often overlooked when evaluating the overall corrosion resistance of products **[5]**.

Traditionally, the corrosion resistance of steel and alloys has been evaluated through long-term exposure tests in natural environments, such as forests and coastal areas. These tests aim to replicate real external conditions, but are time-consuming and often require years or even decades to yield meaningful results. To

† Corresponding Author (ORCID: http://orcid.org/0000-0002-6700-6234): Professor, Department of Mechanical System Engineering, Gyeongsang National University, 2 Tongyeonghaean-ro, Tongyeong, 53064, Korea, E-mail: jh.yagi@gnu.ac.kr, Tel: +82-55-772-9107
1 Professor, Division of Marine Mechatronics, Mokpo National Maritime University, E-mail: k.yeonwon@mmu.ac.kr, Tel: +82-61-240-7237
2 Ph. D. Candidate, Department of Mechanical System Engineering, Gyeongsang National University, E-mail: sdyun@gnu.ac.kr, Tel: +82-55-772-9107
3 Ph. D. Candidate, Department of Mechanical System Engineering, Gyeongsang National University, E-mail: iy76.park@gmail.com, Tel: +82-55-772-9107
4 Professor, Department of Mechanical System Engineering, Gyeongsang National University, E-mail: kimbs@gnu.ac.kr, Tel: +82-55-772-9107

accelerate the evaluation process, researchers and engineers have developed corrosion tests that simulate specific environmental conditions and hasten the corrosion process **[6][7]**.

Common methods for accelerated corrosion testing include salt spray test, immersion, and electrochemical polarization tests. The electrochemical polarization test provides quantitative results and is useful for studying the fundamental electrochemical behavior of materials. However, it has limitations in evaluating large surface areas and is not practical for assessing sectional corrosion, such as that occurring at cut edges. On the other hand, salt spray tests and cyclic corrosion tests (CCT) are widely used for evaluating the corrosion resistance of large surface areas. Despite their widespread evaluation, these methods still lack standardized procedures for assessing sectional corrosion, particularly at cut edges **[8][9]**.

In recent years, image processing technology has emerged as a valuable tool for the nondestructive analysis of the extent of corrosion. Image processing enables the precise and objective assessment of corrosion, providing a detailed understanding of how corrosion progresses over time **[10]**. In this study, we conducted corrosion tests on galvanized ZAM alloy specimens with untreated cut edges. We acquired images of the corroded cut edges and analyzed them using advanced image processing techniques, specifically the grab-cut algorithm and hue, saturation, value (HSV) color space **[11][12]**. This innovative approach enables an objective assessment of corrosion rates and is expected to contribute significantly to the understanding of cut edges, offering valuable insights into sectional corrosion that traditional methods may overlook. Using image processing technology, we aimed to provide a more comprehensive and accurate evaluation of the corrosion resistance, which can provide better material selection and protective strategies in various industrial applications.

2. Experimental Method

2.1 Cyclic corrosion test (CCT)

1) Specimen

Specimens of hot-dip galvanized (HGI) and ZAM steels were prepared to compare their corrosion resistances.

Each specimen had a width, length, and thickness of 10 mm, 15 mm, and 1 mm, respectively. The compositions of the ZAM specimens are listed in **Table 1**.

2) Test Specifications

The corrosion evaluation of the specimens was conducted using ISO 14993 compliant equipment (Q-FOG CCT-600, Q-lab).

Table 1: Composition of ZAM specimens

Specimen \ Composition	Zn (at%)	Mg (at%)	Al (at%)
ZAM	83%	5%	12%

Table 2: CCT conditions for each cycle

Cycle \ Conditions	Time	Temperature	Humidity
Spray conditions	2 h	35°C±1°C	
Dry conditions	4 h	60°C±1°C	<30%
Wet conditions	2 h	50°C±1°C	>95%

The evaluation regimen comprised 100 cycles, with specimens analyzed under a microscope every 10 cycles, starting from the 40th cycle. The detailed cycle conditions are listed in Table 2, which lists the testing parameters and procedures employed in the experiment.

The ISO 14993 standard was adhered to throughout the experiment, specifying a cycle consisting of 2 h of spraying, followed by 4 h of dry conditions and concluding with 2 h of wet conditions, totaling 8 h per cycle. In this study, the NaCl concentration was maintained at 1% or lower to minimize the influence of Cl ions.

2.2 Analysis and Evaluation of Specimens

1) SEM, EDS

Scanning electron microscopy (FE-SEM, Mira3 LM, TESCAN) and energy-dispersive spectrometry (EDS) were employed to examine the cross-section and elemental composition of the specimens following the composite corrosion test.

For image processing, the specimens were intermittently removed every 10 cycles from the 40th to 100th cycle during the composite corrosion test. Subsequently, the cross-sectional images were captured using a microscope. These images were analyzed using a program developed with the OpenCV library in Python. The program aimed to delineate the corroded area of the specimen and assess the distribution of the HSV colors within the corroded region.

3. Results and Discussion

3.1. CCT Results

The corrosion image at the cut edge after 40–100 CCT cycles is shown in **Figure 1**. No discernible corrosion was detected until the 40th cycle. From the 50th cycle onward, yellowish corrosion products appeared along the cut-edge regions. By the 60th cycle, the corroded areas exhibited a transition in coloration toward a brownish hue, accompanied by a gradual increase in the affected surface area.

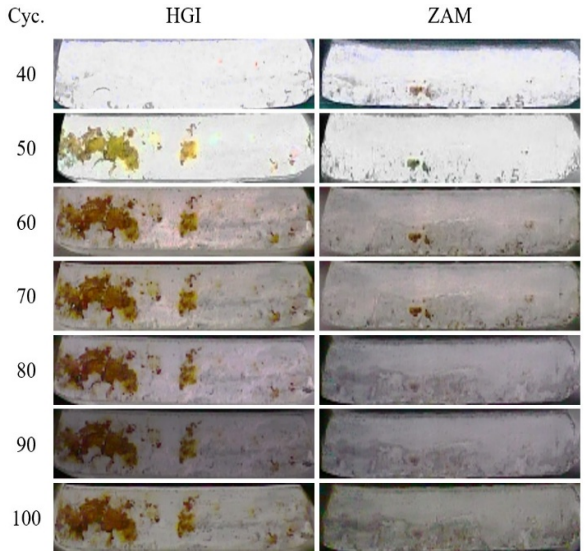

Figure 1: Cut-edge image of specimens after CCT

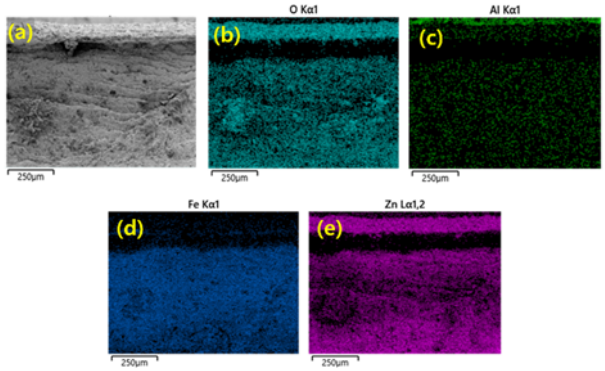

Figure 2: EDS mapping of HGI specimen cut-edge, including SEM image (a), O element (b), Al element (c), Fe element (d), Zn element (e)

With a further progression of the cycles, the corrosion products continued to evolve in appearance, ultimately developing a characteristic reddish-brown coloration.

In the ZAM specimens, minor reddish corrosion was observed at the 40th cycle. In addition, localized color changes were detected near small scratches in the cut-edge region. By the 60th cycle, the coloration of the corroded areas shifted to a yellowish tone, and after the 80th cycle, it further transitioned to a whitish appearance. Overall, the ZAM specimens exhibited a tendency in which the corroded area did not expand, but rather decreased with increasing cycles, even after the initiation of corrosion.

In particular, for the ZAM specimen, the reddish brown region, likely composed of iron oxide, began to diminish in size from the 80th cycle onward. This phenomenon is attributed to the action of the corrosion product simonkolleite in the ZAM specimens, which functions as a protective film covering the initially formed iron oxide region.

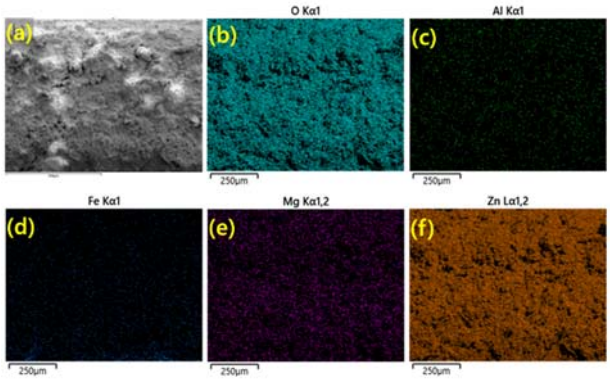

Figure 3: EDS mapping of ZAM specimen cut-edge, including SEM image (a), O element (b), Al element (c), Fe element (d), Mg element (e), Zn element (f)

3.2 SEM and EDS Analysis

The FE-SEM and EDS images of the HGI specimen after CCT exposure are shown in **Figure 2**.

The EDS results confirmed that the cut edge of the HGI specimen was predominantly covered with a Zn-rich phase. The elemental distribution revealed a continuous Zn signal along the cut edge accompanied by a relative decrease in the Fe signal from the substrate. These observations suggest that, as corrosion progressed from the galvanized Zn layer, zinc corrosion products migrated along the cut edge through electrolyte transport and capillary action and were subsequently redeposited to form a covering layer over the exposed area.

Figure 3 shows the FE-SEM and EDS results for the ZAM specimen. Compared with the HGI specimen, Zn, Mg, and Al were detected on the cut-edge surface of the ZAM specimen after CCT, indicating the presence of corrosion products derived from the alloyed coating elements. Moreover, the results demonstrate that, with the progression of the CCT, these corrosion products progressively migrated and accumulated, eventually forming a continuous layer that covered the cut-edge surface.

These results indicate that the cut-edge corrosion behavior is governed not only by the zinc coating itself but also by the stability and mobility of the corrosion products formed. In the ZAM specimen, the Mg- and Al-containing corrosion products remained adhered to the cut edge and contributed to the sustained surface coverage during CCT exposure.

In particular, the EDS mapping results reveal that the ZAM specimen exhibited a lower proportion of base metal Fe than the HGI specimen, indicating that the exposed Fe was more extensively masked by the corrosion products. As further evidenced by the FE-SEM images of the ZAM specimen, the

Table 3: Corrosion area of each specimen over 40–100 CCT cycles

Cyc.	40	50	60	70	80	90	100
HGI	0.17	27.13	45.85	36.78	31.16	28.94	27.96
ZAM	1.12	6.15	8.96	9.47	1.14	1.11	0.65

corrosion products enriched with Zn, Mg, and Al migrated and subsequently formed a covering layer on the cut-edge surface.

3.3 Analyzing Corrosion Images with Image Processing

Based on the results shown in **Figure 1**, after CCT, the images were analyzed using an image processing technique. **Table 3** presents the corrosion area ratios of each specimen calculated using image processing. The image processing method employed in this study first applied the grab-cut technique to extract the region of interest from the images. The initial grab-cut seeds and the HSV thresholds were determined from preliminary images by manually labeling corroded regions and extracting their color distribution. The extracted images were then converted into the HSV color space, and pixels corresponding to the reddish color range, which is characteristic of the corrosion products of Fe used as the base metal, were identified as the corrosion area. To ensure a quantitative evaluation, the number of pixels classified as corrosion was divided by the total pixel count of the extracted region, thereby providing the corrosion area ratio. This approach enables the differentiation of corroded regions from unaffected areas with improved consistency, even with complex surface morphologies.

Figures 4 and **5** show the corrosion areas detected using the image processing method for the HGI and ZAM specimens, respectively. In both the HGI and ZAM specimens, rust formation was first detected after cycle 40, with the corroded area progressively increasing up to 50–60 cycles in the HGI specimen and 70 cycles in the ZAM specimen, as confirmed by image processing analyses. However, after these cycles, both specimens exhibited a reduction in the proportion of corroded surfaces. This behavior is presumed to be associated with the dissolution and detachment of corrosion products, as well as the subsequent coverage of the cut edge by the redeposited coating-derived phases, which diminished the detectable intensity of the reddish coloration typical of iron oxide. These findings suggest that the progression of corrosion is influenced not only by the initiation and expansion of rust but also by the redistribution and masking effects of corrosion products, thereby emphasizing the evolving characteristics of corrosion morphology under prolonged CCT exposure.

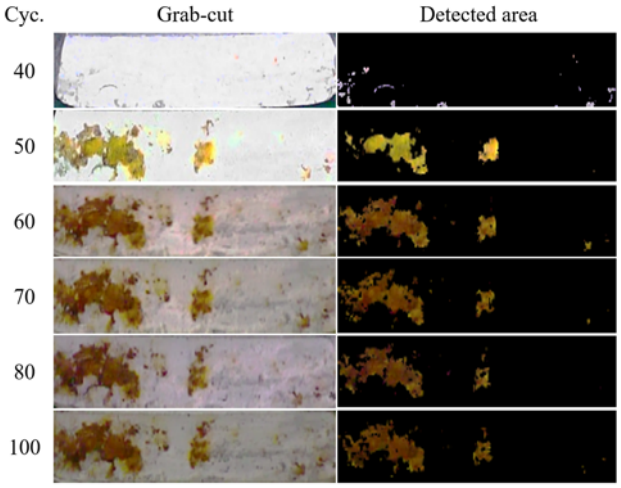

Figure 4: Corrosion detection image of the HGI specimen obtained through image processing

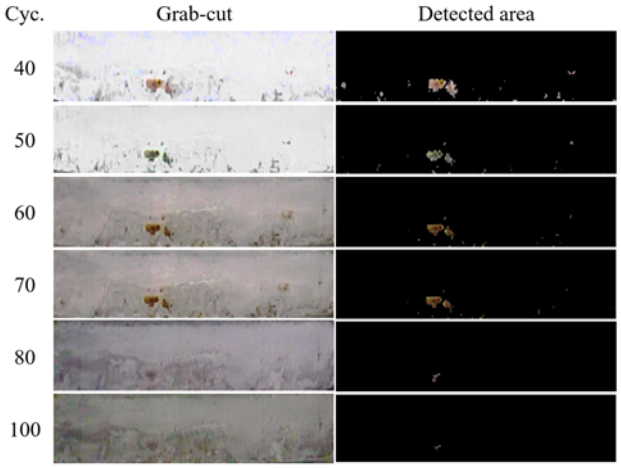

Figure 5: Corrosion detection image of the ZAM specimen obtained through image processing

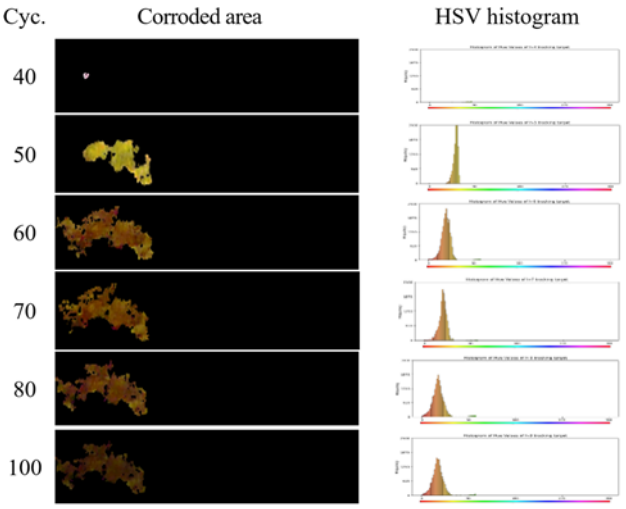

Figure 6: HSV histogram of the HGI specimen at the corroded area obtained through image processing

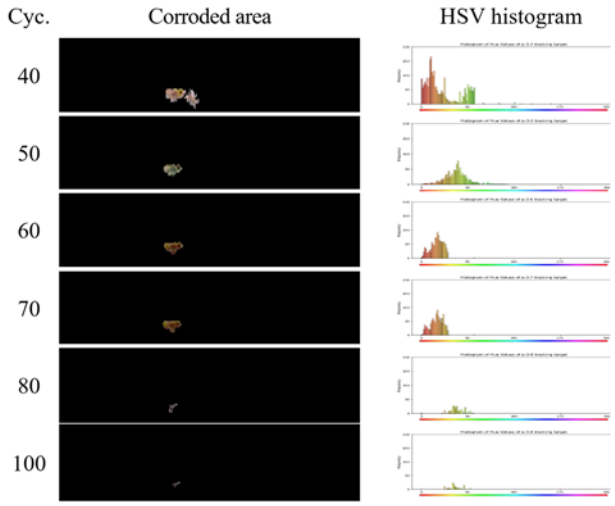

Figure 7: HSV histogram of the ZAM specimen at the corroded area

Figures 6 and **7** show the HSV histograms of the rusted areas for the HGI and ZAM specimens, respectively. For the HGI specimen, the histogram at cycle 50 showed a dominant yellow region, which gradually shifted toward the red region as the cycles progressed, accompanied by a broadening of the overall color distribution. This observation is consistent with the results in **Figure 4**, where the reddish coloration became less pronounced as the galvanized layer progressively covered the cut edge during CCT. This is further supported by the EDS analysis, indicating the influence of zinc.

In contrast, the ZAM specimen exhibited reddish regions after the initial 40 cycles; however, with further cycling, the distribution shifted toward the yellow and green regions. This behavior can be attributed to the protective properties of the corrosion-resistant Zn-Mg-Al ternary alloy layer, which reduced the detectable intensity of reddish rust even when corrosion was initiated at the cut edge as the coating film continued to provide coverage. Moreover, the overall color intensity gradually decreased.

Taken together, these findings suggest that the evolution of the HSV color regions can serve as an indirect indicator of corrosion progression, simultaneously reflecting the transformation of corrosion products and the protective effects of galvanized and alloyed coating layers.

4. Conclusion

This study observed and analyzed the cut-edge corrosion behaviors of HGI and ZAM specimens. Through a CCT, it was visually confirmed that the corrosion area at the cut edge of the ZAM specimen decreased as the test cycles progressed, which was attributed to the protective action of the corrosion product, simonkolleite. In addition, SEM and EDS analyses revealed that the corrosion products descending from the surface effectively covered the cut edge, thereby acting as protective barriers to the base metal.

Furthermore, it was confirmed that image processing techniques enabled the quantitative monitoring of corrosion images, providing measurable indicators of corrosion progression. The variations in color regions identified through image processing are presumed to serve not only as changes in appearance but also as indicators reflecting both the degree of corrosion progression and the protective function of the coating layer.

Acknowledgement

This work was supported by the Gyeongsang National University Fund for Professors on Sabbatical Leave, 2023.

Author Contributions

Conceptualization, J. Yang; Methodology, S. D Yun and I. Park; Investigation, S. D Yun, B. Kim, Y. Kim; Resources, J. Yang; Data Curation S. D Yun and B. Kim; Writing-Original Draft Preparation, Y. Kim and S. D Yun; Writing-Review & Editing, Y. Kim and J. Yang; Visualization, Y. Kim; Supervision, J. Yang; Project Administration, J. Yang; Funding Acquisition, J. Yang.

References

[1] B. Kim, Y. Kim, and J. Yang, “Detection of corrosion on steel plate by using image segmentation method,” Corrosion Science and Technology, vol. 54, no. 2, pp. 84–89, 2021(in Korean).

[2] J. -W. Lee, S. -Y. Oh, B. Park, M. -S. Oh, and S. J. Kim, “Corrosion behaviors of the Eutectic structure in Zn–Al–Mg alloy coated steel in chloride containing aqueous environment,” Korean Journal of Metals and Materials, vol. 58, no. 9, pp. 610-616, 2020 (in Korean).

[3] J. Kou and D. Ma, “Galvanic corrosion based on wire beam electrode technique: progress and prospects,” Corrosion Reviews, vol. 40, no. 3, pp. 423-442, 2022.

[4] J.-W. Lee, B. R. Park, S.-Y. Oh, D.W. Yun, J. K. Hwang, M.-S. Oh, and S. J. Kim, “Mechanistic study on the cut-edge corrosion behaviors of Zn–Al–Mg alloy coated steel sheets in

chloride containing environments," Corrosion Science, vo. 160, p. 110886, 2019.

[5] S. Tokuda, Y. Nishida, M. Nishimoto, I. Muto, and H. Shoji, "Initial dissolution of Mg-containing phase and corrosion product formation in cut-edge corrosion of Zn–11%Al–3%Mg–0.2%Si coated steel," Corrosion Science, vol. 225, p. 111605, 2023.

[6] K. Kapfer, M. Mandel, A. Mittelbach, and L. Kruger, "Investigation and modelling of edge corrosion of e-coated galvanized steel with respect to the spatial edge orientation," Materials and Corrosion, vol. 73, pp. 55-67, 2022.

[7] M. F. Bolsanello, A. A. García, L. X. da C. Lima, B. K. Neto, J. L. Ferreira, J. L. Rossi, I. Costa, R. M. Souto, and J. Izquierdo, "Contributions to a more realistic characterization of corrosion processes on cut edges of coated metals using scanning microelectrochemical techniques, illustrated by the case of ZnAlMg-galvanized steel with different coating densities," Materials, vol. 17, no. 7, 1679, 2024.

[8] S. Sheikholeslami, G. Williams, H. N. McMurray, L. Gommans, S. Morrison, S. Ngo, D. E. Williams, and W. Gao, "Cut-edge corrosion behavior assessment of newly developed environmental-friendly coating systems using the scanning vibrating electrode technique (SVET)," Corrosion Science, vol. 192, 109813, 2021.

[9]S. -H. Kim, S. -Y. Jin, J. -H. Yang, and Y. -S. Yun, "Self-healing phenomenon at the cut edge of Zn–Al–Mg alloy coated steel in chloride environments," Coatings, vol. 14, no. 4, 485, 2024.

[10] T. T. Nguyen, S. Akbarzadeh, T. T. Thai, Y. Paint, A. Truc Trinh, M.-G. Olivier, "Effect of cerium salts on the cut-edge corrosion behavior of zinc-based alloy coatings," Journal of Alloys and Compounds, vol. 981, p. 173711, 2024.

[11] T. Gu, Y. Liu, C. Peng, P. Zhang, and Z. Wang, "Initial atmospheric corrosion of zinc-aluminum-magnesium coated steel and galvanized steel in regions of extremely cold and industrial climate," Materials Chemistry and Physics, vol. 291, 126686, 2022.

[12] A. Kobayashi, K. Norita, T. Yasutomi, "Cutting technologies to improve early corrosion resistance on the cut edge of galvanized steel sheets," Nippon Steel Technical Report, vol. 129, pp. 72–78, 2023.